Print ISSN: 2321-6379
Online ISSN: 2321-595X

Original Article

Role of Diffusion-weighted Imaging, Perfusion Magnetic Resonance Imaging, and Magnetic Resonance Spectroscopy in Evaluating Histopathologically Confirmed Brain Tumors in 3-Tesla Magnetic Resonance Imaging

Deepak Jain[1], Satya Bhuwan Singh Netam[2], Vivek Patre[3], Dnyanesh Amle[4], Rajiv Sahu[5], Renuka Gahine[6]

[1]Assistant Professor, Department of Radiology, Pt. Jawahar Lal Nehru Memorial Medical College, Raipur, Chhattisgarh, India, [2]Professor, Department of Radiology, Pt. Jawahar Lal Nehru Memorial Medical College, Raipur, Chhattisgarh, India, [3]Professor, Department of Radiology, Pt. Jawahar Lal Nehru Memorial Medical College, Raipur, Chhattisgarh, India, [4]Assistant Professor, All India Institute of Medical Sciences, Nagpur, Maharashtra, India, [5]Associate Professor, Department of Neurosurgery, Pt. Jawahar Lal Nehru Memorial Medical College, Raipur, Chhattisgarh, India, [6]Professor and Head, Department of Pathology, Pt. Jawahar Lal Nehru Memorial Medical College, Raipur, Chhattisgarh, India

Abstract

Objective: Our aim was to evaluate the diagnostic capabilities of physiological magnetic resonance imaging (MRI) in differentiating type and grades of tumor and correlation with prospective histopathology results.

Materials and Methods: We evaluated 70 patients in 3-tesla MRI preoperatively using conventional and physiological MR sequences (diffusion, perfusion, and spectroscopy) of common brain tumors who were prospectively confirmed by histopathology. Post-imaging analysis was done by available software and ratio was calculated. Data were expressed as mean ± standard deviation and median (range) and Kolmogorov–Smirnov analysis was used to check distribution. Multiple statistical tests were applied and receiver operating characteristic (ROC) curve was plotted wherever feasible.

Results: We obtained a significant difference in spectroscopic parameters, relative cerebral blood volume, and apparent diffusion coefficient values between different tumor groups and also between different tumor grades. ROC curve plotted among groups showed sensitivity and specificity of diagnostic capability. Time-intensity curve showed a significant difference between different tumor groups and correlation with grades of tumor.

Conclusion: We propose an algorithm for differentiating different types and grades of common brain tumor using physiological MRI in addition to conventional MR sequences.

Key words: 3-tesla magnetic resonance imaging, Apparent diffusion coefficient, Magnetic resonance spectroscopy, Perfusion magnetic resonance imaging

INTRODUCTION

Imaging plays a crucial role in the management of brain tumors. Magnetic resonance imaging (MRI) has the most potential of any imaging technique to allow a complete and accurate diagnosis and initial management strategy to be formulated for a brain tumor. Although MRI has delivered remarkable advances in the information available from the vast array of pulse sequences and MRI techniques, the radiologist still relies most heavily on more fundamental criteria's, such as location in the neuraxis and the age of the patient, for specific pathologic diagnoses.

Apart from conventional sequences, physiological MRI such as diffusion-weighted (DW) imaging, perfusion MRI (pMRI), and proton MR spectroscopy, provides additional

Access this article online

www.ijss-sn.com

Month of Submission : 03-2019
Month of Peer Review : 04-2019
Month of Acceptance : 04-2019
Month of Publishing : 05-2019

Corresponding Author: Dr. Deepak Jain, Department of Radiology, Pt. Jawahar Lal Nehru Memorial Medical College, Raipur - 492 001, Chhattisgarh, India.

Table 1: General characteristics of study subjects

Characteristics	Value (Mean ± SD) *n* (%)
Age (Years)	38.67±17.79
Gender	
Male	33 (47.14)
Female	37 (52.86)
Volume (cc)	95.09±127.57
2D MR NAA/Cr	0.70±0.57
2D MR Cho/Cr	4.29±3.18
SVS NAA/Cr	1.55±1.80
SVS Cho/Cr	3.94±3.45
SVS Iac/Cr	2.76±5.22
SVS Mi/Cr	1.65±3.01
SVS Glu/Cr	0.82±1.94
ADC value	1041.43±257.51
rCBV	3.95±2.59
% regain in signal intensity	
21–40	28 (39.91)
41–60	21 (30.00)
61–80	18 (25.71)
81–100	3 (4.29)
Tumor type	
Astrocytic tumors	30 (42.86)
Cranial nerve tumors	9 (12.86)
Meningothelial tumors	15 (21.43)
Metastasis	5 (7.14)
Oligodendroglial tumors	3 (4.29)
Others	8 (11.43)
Grade of tumor	
I	33 (47.14)
II	17 (24.29)
III	5 (7.14)
IV	10 (14.29)
Metastasis	5 (7.14)

information regarding grade, type of tumor, vascularity, and composition. This is a study to find out the utility of physiological MRI in brain tumors, in 3-tesla (3T) MRI with an emphasis on its capabilities to differentiate the type of tumor, grade of tumor, and to some extent prognosis of the tumor and its histopathological correlation.

MATERIALS AND METHODS

We did our study at the Department of Radiology, Pt. Jawahar Lal Nehru Memorial Medical College, Raipur, Chhattisgarh, for a period extending from July 2014 to March 2018. Patients having primary brain neoplasm or metastasis who are later confirmed histopathologically are selected for the study. Informed consent was taken from all the patients who were enrolled for the study. Patients who are unwilling to take part in the study or who are histologically proven non-tumorous intra-cerebral lesion or patients who are already treated for brain tumors were excluded from the study. The data for the study were collected through a uniform pro forma. We used Magnetom Skyra MRI machine and accessories having 3-T field strength with 70 cm open bore design and 173 cm system length. Radiofrequency Tim (204 × 48) (204 × 64) (204 × 128) was used with gradient strength – XQ Gradients (45 mT/m at 200T/m/s) and zero Helium boil-off technology. The contrast was given through pressure injector.

DW images were obtained using an axial echo-planar spin echo (SE) sequence (4700/98 ms (repetition time [TR]/ echo time [TE]), on average, 4-mm section thickness, 288 × 360 matrix size, 220 × 220-mm FOV) in 22 s. DW images and apparent diffusion coefficient (ADC) maps were acquired at b values 0, and 1000 s/mm^2. No obvious post-processing was required. Solid appearing tumoral areas were sampled manually. Standard mean ADC values were calculated by the manual drawing of the region of interest (ROI) circle and expressed in 10^{-3} mm^2/s. Control ADC values were obtained from normal-appearing white matter from contralateral normal brain tissue.

The contrast was administered using 18–20 gauge intravenous catheter through pressure injector. We used a susceptibility T2*-weighted multi-slice multi-shot fast field echo-echo-planar imaging (EPI) sequence with water selective excitation pre-pulse. The imaging parameters were as follows: 1650/30 ms TR/TE; 90° flip angle; 1 excitation; 221 × 221 mm FOV; 4 mm section thickness; 128 × 128 reconstruction matrix; 1.7 × 1.7 × 4.0 mm voxel size; 0% intersection gap; 1220 signal intensity bandwidth in EPI readout direction; and 128 EPI factor; keeping phase Fourier transformation off. 25 sections were obtained without intersection gap to cover the entire lesion volume identified on T2-weighted images. A series of 50 multi-section acquisitions were acquired at 1.84 s intervals, the total acquisition time is 1 min 32 s. The first six acquisitions are performed before the contrast agent injection to establish a pre-contrast baseline. At the seventh acquisition, 0.2 mmol/kg of body weight of gadodiamide (Omniscan; GE Healthcare Pvt. Ltd. IDA Business Park, Carrigtohill. Cork, Ireland) was injected with a power injector at a rate of 4 mL/s through an 18- or 20-gauge intravenous catheter, immediately followed by a bolus injection of saline at the same rate for a total of 20 ml. Axial contrast-enhanced T1-weighted images were obtained after the perfusion images, using the same parameters as for the pre-contrast images.

The DSC perfusion images were transferred to Syngo through (workstation-Siemens Medical Systems). Image analysis and measurements were performed with T2* perfusion tool software. The raw data were processed off-line. A motion correction of 3 mm was applied to raw images before integration. During the first pass of the bolus of paramagnetic contrast material, the signal intensity in T2*-weighted sequence decreased, whereas the signal intensity partially restored directly after the passage.

Table 2: Comparison of various radiological parameters between subjects with a different type of tumor

Radiological characteristics	Mean±SD	Std. error	f/Chi-square	*P* Value
Volume				
Astrocytic tumors	124.26±163.56	34.10	26.99#	<0.0001
Cranial nerve tumors	52.91±16.74	5.58		
Meningothelial tumors	45.43±22.71	6.07		
Metastasis	13.52±7.37	3.29		
Oligodendroglial tumors	363.88[a, b, c, d, f]±14.58	8.42		
Others	95.86±98.44	37.21		
2D MR NAA/Cr				
Astrocytic tumors	0.63±0.28	0.05	4.107*	0.003
Cranial nerve tumors	1.35[a]±0.76	0.25		
Meningothelial tumors	0.63[b]±0.29	0.07		
Metastasis	0.31[b]±0.18	0.08		
Oligodendroglial tumors	0.25[b]±0.06	0.03		
Others	0.75±1.10	0.39		
2D MR Cho/Cr				
Astrocytic tumors	3.13±1.53	0.28	3.144*	0.013
Cranial nerve tumors	3.45±0.62	0.21		
Meningothelial tumors	6.46[a]±4.82	1.24		
Metastasis	3.93±0.06	0.03		
Oligodendroglial tumors	6.69±0.03	0.02		
Others	4.88±4.85	1.72		
SVS NAA/Cr				
Astrocytic tumors	0.99±0.82	0.20	9.244#	0.10
Cranial nerve tumors	3.28±3.70	1.31		
Meningothelial tumors	1.01±0.83	0.23		
Metastasis	1.60±0.05	0.02		
Oligodendroglial tumors	0.62			
Others	1.92±1.36	0.48		
SVS Cho/Cr				
Astrocytic tumors	3.02±3.22	0.81	16.54#	0.005
Cranial nerve tumors	3.14±1.64	0.58		
Meningothelial tumors	6.15±3.00	0.83		
Metastasis	0.64±1.43	0.64		
Oligodendroglial tumors	5.82			
SVS Iac/Cr				
Astrocytic tumors	2.88±3.17	0.79	11.80#	0.038
Cranial nerve tumors	0.00±0.00	0.00		
Meningothelial tumors	1.88±1.75	0.50		
Metastasis	1.98±0.04	0.02		
Oligodendroglial tumors	0.62			
Others	7.05±11.39	4.03		
SVS Mi/Cr				
Astrocytic tumors	0.63±1.15	0.30	17.207#	0.002
Cranial nerve tumors	5.47±3.14	1.11		
Meningothelial tumors	1.28±3.78	1.09		
Metastasis	0.00±0.00	0.00		
Oligodendroglial tumors				
Others	1.31±2.19	0.77		
SVS Glu/Cr				
Astrocytic tumors	0.03±0.09	0.03	15.643#	0.004
Cranial nerve tumors	3.83±2.61	0.99		
Meningothelial tumors	0.81±2.00	0.58		
Metastasis	0.00±0.00	0.00		
Oligodendroglial tumors				
Others	0.03±0.09	0.03		
ADC value				
Astrocytic tumors	1053.63±285.39	52.11	2.309*	0.054
Cranial nerve tumors	1064.78±98.39	32.80		
Meningothelial tumors	1084.13±178.56	46.10		
Metastasis	685.60[a,c]±13.18	5.90		
Oligodendroglial tumors	1079.67±150.34	86.80		
Others	1097.38±367.34	129.87		

(Contd...)

Table 2: *(Continued)*

Radiological characteristics	Mean±SD	Std. error	f/Chi-square	*P* Value
rCBV				
Astrocytic tumors	3.82±2.05	0.38	2.521*	0.038
Cranial nerve tumors	2.91±0.41	0.14		
Meningothelial tumors	5.79±3.89	1.00		
Metastasis	2.58±0.08	0.04		
Oligodendroglial tumors	2.77±0.12	0.07		
Others	3.49±2.66	0.94		

*f, #Chi-square, [a]*P*<0.05 versus Astrocytic tumors, [b]*P* < 0.05 versus Cranial nerve tumors, [c]*P* < 0.05 versus Meningothelial tumors, [d]*P* < 0.05 versus Metastasis, [e]*P* < 0.05 versus Oligodendroglioma, [f]*P* < 0.05 versus others, rCBV: Relative cerebral blood volume, Adc: Apparent diffusion coefficient, ROI: Region of interest, EPI: Echo-planar imaging, TSIC: Time signal intensity curve, SVS: Single-voxel spectroscopy, 2D-MVS: 2D multivoxel spectroscopy, NAA: N-acetyl aspartate, Cho: Choline compounds, Cr: Creatine, : Alanine, Mimyo-inositol, Glu: Glutamine, lac: Lactate

Table 3: Comparison of various radiological parameters between subjects with different grade of the tumor

Radiological characteristics	Mean±SD	Std. error	f/Chi-square	*P* value
Volume				
I	77.60±70.74	12.71	14.49	0.006
II	119.29±128.04	32.01		
III	101.45±36.54	16.34		
IV	227.83±388.14	194.07		
Metastasis	13.52±7.37	3.29		
2D MR NAA/Cr				
I	0.87±0.73	0.13	2.062	0.096
II	0.64±0.35	0.09		
III	0.33±0.27	0.12		
IV	0.62±0.14	0.05		
Metastasis	0.31±0.18	0.08		
Total	0.70±0.57	0.07		
2D MR Cho/Cr				
I	4.79±4.31	0.75	0.816	0.519
II	4.46±2.00	0.49		
III	3.81±0.04	0.02		
IV	2.78±0.80	0.25		
Metastasis	3.93±0.06	0.03		
Total	4.29±3.18	0.38	11.84	0.019
SVS NAA/Cr				
I	1.95±2.31	0.44		
II	0.63±0.72	0.25		
III	0.66±0.29	0.17		
IV	1.45±0.90	0.32		
Metastasis	1.60±0.05	0.02		
SVS Cho/Cr				
I	5.34±3.79	0.73	14.11	0.007
II	3.43±2.82	1.00		
III	4.01±1.33	0.77		
IV	1.79±1.19	0.42		
Metastasis	0.64[a]±1.43	0.64		
SVS lac/Cr				
I	2.69±6.66	1.33	9.49	0.05
II	1.71±4.05	1.43		
III	2.12±3.14	1.81		
IV	4.80±3.03	1.07		
Metastasis	1.98±0.04	0.02		
SVS Mi/Cr				
I	2.77±3.68	0.72	14.29	0.006
II	0.03±0.07	0.03		
III	2.50±1.95	1.38		
IV	0.24±0.69	0.24		
Metastasis	0.00±0.00	0.00		

(Contd...)

Table 3: *(Continued)*

Radiological characteristics	Mean±SD	Std. error	f/Chi-square	*P* value
SVS Mi/Cr				
I	2.77±3.68	0.72	14.29	0.006
II	0.03±0.07	0.03		
III	2.50±1.95	1.38		
IV	0.24±0.69	0.24		
Metastasis	0.00±0.00	0.00		
SVS Glu/Cr				
I	1.52±2.47	0.50	7.665	0.105
II	0.04±0.10	0.04		
III	0.34			
IV	0.00±0.00	0.00		
Metastasis	0.00±0.00	0.00		
ADC value				
I	1201.33±214.14	37.28	13.245	<0.0001
II	1005.53[a]±234.32	56.83		
III	846.20[a]±76.33	34.14		
IV	850.30a,[b]±129.51	40.95		
Metastasis	685.60a,[b]±13.18	5.90		
rCBV				
I	4.65±3.21	0.56	1.685	0.164
II	3.32±2.04	0.49		
III	2.28±0.05	0.02		
IV	4.09±1.32	0.42		
Metastasis	2.58±0.08	0.04		

rCBV: Relative cerebral blood volume, Adc: Apparent diffusion coefficient, ROI: Region of interest, EPI: Echo-planar imaging, TSIC: Time signal intensity curve, SVS: Single-voxel spectroscopy, 2D-MVS: 2D multivoxel spectroscopy, NAA: N-acetyl aspartate, Cho: Choline compounds, Cr: Creatine, Ala: Alanine, Mimyo-inositol, Glu: Glutamine, lac: Lactate

Table 4: Comparison of various radiological parameters between astrocytic tumors and non-astrocytic tumors

Radiological characteristics	Tumor	Mean±SD	Std. error mean	t/Mann–Whitney U-test	*P* value
Volume	Astrocytic tumors	124.26±163.56	34.10	236.0[b]	0.003
	Other tumors	77.44±98.15	15.92		
2D MR NAA/Cr	Astrocytic tumors	0.63±0.28	0.05	-0.851[a]	0.398
	Other tumors	0.75±0.71	0.11		
2D MR Cho/Cr	Astrocytic tumors	3.13±1.53	0.28	-1.530[a]	0.007
	Other tumors	5.17±3.79	0.60		
SVS NAA/Cr	Astrocytic tumors	0.99±0.82	0.20	222.0[b]	0.239
	Other tumors	1.81±2.06	0.35		
SVS Cho/Cr	Astrocytic tumors	3.02±3.22	0.81	207.0[b]	0.138
	Other tumors	4.36±3.52	0.59		
SVS lac/Cr	Astrocytic tumors	2.88±3.17	0.79	210.5[b]	0.246
	Other tumors	2.71±6.02	1.05		
SVS Mi/Cr	Astrocytic tumors	0.63±1.15	0.30	207.5[b]	0.314
	Other tumors	2.11±3.47	0.60		
SVS Glu/Cr	Astrocytic tumors	0.03±0.09	0.03	169.0[b]	0.162
	Other tumors	1.15±2.22	0.39		
ADC value	Astrocytic tumors	1053.60±285.39	52.11	0.341[a]	0.734
	Other tumors	1032.30±237.81	37.60		
rCBV	Astrocytic tumors	3.82±2.05	0.38	-0.370[a]	0.713
	Other tumors	4.05±2.94	0.47		

[a]: *t*-value, [b]: Mann–Whitney U-test, rCBV: Relative cerebral blood volume, Adc: Apparent diffusion coefficient, ROI: Region of interest, EPI: Echo-planar imaging, TSIC: Time signal intensity curve, SVS: Single-voxel spectroscopy, 2D-MVS: 2D multivoxel spectroscopy, NAA: N-acetyl aspartate, Cho: Choline compounds, Cr: Creatine, Ala: Alanine, Mimyo-inositol, Glu: Glutamine, lac: Lactate

Table 5: Association of percentage regain in signal intensity with different characteristics of the tumor

Characteristics	Chi-square	*P* value
Astrocytic tumors and other tumors	9.063	0.06
Different classes of tumors	38.22	0.008
Grade of tumors	46.95	<0.0001

The relative measure of contrast agent concentration can be calculated from the time signal intensity curve (TSIC).

Single-voxel spectroscopy (SVS) data were obtained using a double SE point-resolved spectroscopy (PRESS) sequence with one-pulse water signal suppression mainly from contrast-

Table 6: ROC curve analysis of primary brain tumors to assess the diagnostic significance of various parameters in identifying intraaxial tumors from extraaxial tumors

AUC								
Test result variable (s)	Area	Std. error[a]	Asymptotic sig.[b]	Asymptotic 95% confidence interval		Cutoff	Sensitivity	Specificity
				Lower Bound	Upper Bound			
2D MR Cho/Cr[a]	0.598	0.095	0.354	0.411	0.786	5.95	29	100
SVS Cho/Cr[a]	0.481	0.105	0.855	0.276	0.685	5.28	32.3	80
SVS lac/Cr[a]	0.650	0.101	0.158	0.452	0.848	0.97	58.1	70
rCBV[a]	0.569	0.102	0.514	0.369	0.770	3.46	45.2	80
2D MR NAA/Cr[b]	0.655	0.115	0.164	0.431	0.880	068	69	66.7
SVS NAA/Cr[b]	0.584	0.111	0.450	0.367	0.801	0.77	34.5	88.9
SVS Mi/Cr[b]	0.705	0.118	0.066	0.474	0.936	2	93.1	55.6
SVS Glu/Cr[b]	0.684	0.119	0.099	0.452	0.916	5.32	100	44.4
ADC value[b]	0.590	0.105	0.420	0.383	0.797	1003	55.2	77.8

[a]: Positive if more than, [b]: Positive if less than, rCBV: Relative cerebral blood volume, Adc: Apparent diffusion coefficient, ROI: Region of interest, EPI: Echo-planar imaging, TSIC: Time signal intensity curve, SVS: Single-voxel spectroscopy, 2D-MVS: 2D multivoxel spectroscopy, NAA: N-acetyl aspartate, Cho: Choline compounds, Cr: Creatine, Ala: Alanine, Mimyo-inositol, Glu: Glutamine, lac: Lactate, ROC: Receiver operating characteristic, AUC: Area under the curve

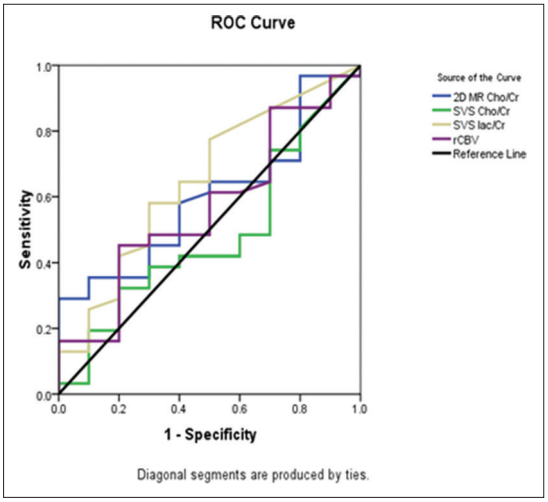

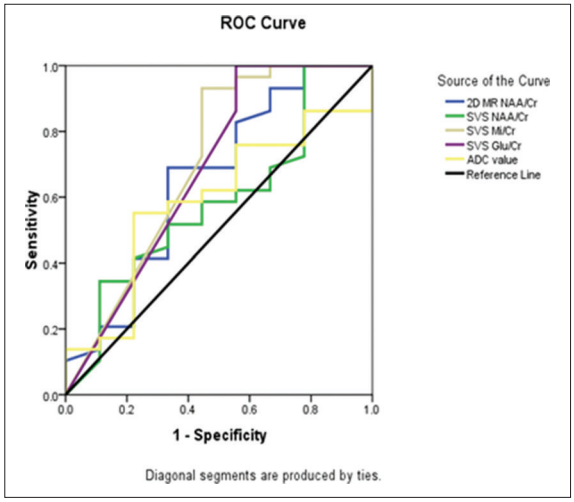

enhanced areas of the lesions, while avoiding contamination. Spectroscopic data from cubic volumes of 2 × 2×2 cm^3 were obtained using the PRESS sequence with 2000/30 ms (TR/TE), 80 averages, 1024 data points, and 1200 Hz spectrum width. The acquisition time was approximately 2 min 50 s. 2D multivoxel spectroscopy (2D-MVS) data were obtained using a chemical shift imaging with a water suppression pulse sequence mainly from metabolically active fleshy parts of the lesions, while avoiding contamination from scalp fat. Spectroscopic data from cubic volumes of 8 × 8×1.5 cm^3 were obtained by using the PRESS sequence (csi_slaser: Siemens) containing 64 voxels and each voxel measuring 1 × 1×1.5 cm^3 with 1700/135 ms (TR/TE), 3 averages, 1024 data points, and 1200 Hz spectrum width. The acquisition time was approximately 6 min 53 s. Appropriate automatic shimming and water suppression were achieved using 50 Hz bandwidth, no spectral width, and the automated software developed by the manufacturer for SVS and 2D-MVS both. The time domain signal intensity was optimized and processed to remove the residual water signal. Post-processing of the spectroscopic data consisted of frequency shift and phase and linear baseline corrections after Fourier transformation. These processes were automatic mostly, but manual processing was done whenever needed. Frequency domain curve was fitted to Gaussian line shape using the software provided by the manufacturer to analyze different metabolic peaks. Metabolic peaks used in the differentiation of the different tumor types were as follows: N-acetyl aspartate (NAA) at 2–2.1 parts per million (ppm), Choline (Cho) at 3.2–3.3 ppm, Creatine (Cr) at 3–3.1 ppm, and lipid-containing compounds in the range of 0.9–1.3 ppm. Other metabolic peaks, if any, were also calculated as alanine (Ala) at 1.4–1.6 ppm, myo-inositol (Mi) at 3.6–3.8 ppm, glutamine (Glu) at 2.1–2.3 ppm, and lactate (lac) at 1.3 ppm. Metabolite values were calculated automatically from the area under each metabolite peak using the standard commercial software program provided by the manufacturer. Peak integral values were normalized to the internal Cr peak. Metabolite ratios of NAA/Cho, NAA/Cr, Cho/Cr, and if possible, Mi/Cr, Ala/Cr, lac/Cr, and Glu/Cr were calculated.

We evaluated relative cerebral blood volume (rCBV) and TSIC of pMRI and drew all ROI with consensus

Table 7: Diagnostic potential and diagnostic cutoff of various radiological parameters to diagnose meningo epithelial tumors from astrocytoma

Test result variable (s)	AUC	Std. error[a]	*P* value	95% CI		Cutoff	Sensitivity	Specificity
				Low	High			
Volume[b]	0.448	0.089	0.617	0.273	0.624	17.86	100	24.1
2D MR NAA/Cr[b]	0.649	0.100	0.150	0.454	0.844	0.61	81.8	62.1
2D MR Cho/Cr[b]	0.746	0.103	0.017	0.545	0.947	4.69	81.8	79.3
SVS Cho/Cr[b]	0.793	0.073	0.005	0.650	0.936	4.675	90.9	72.4
SVS lac/Cr[b]	0.636	0.089	0.188	0.462	0.811	0.37	90.9	51.7
ADC value[b]	0.607	0.090	0.303	0.430	0.783	845	100	34.5
rCBV[b]	0.671	0.114	0.099	0.447	0.895	5.98	54.5	93.1
SVS NAA/Cr[a]	0.691	0.084	0.053	0.526	0.856	1.11	91.7	60.6
SVS Mi/Cr[a]	0.576	0.095	0.441	0.389	0.762	1.54	91.7	30.3
SVS Glu/Cr[a]	0.518	0.098	0.857	0.325	0.710	4.29	91.7	15.2

[a]: positive if lesser than or equal to, [b]: Positive if greater than or equal to, AUC: Area under the Curve, CBV: Relative cerebral blood volume, Adc: Apparent diffusion coefficient, ROI: Region of interest, EPI: Echo-planar imaging, TSIC: Time signal intensity curve, SVS: Single-voxel spectroscopy, 2D-MVS: 2D multivoxel spectroscopy, NAA: N-acetyl aspartate, Cho: Choline compounds, Cr: Creatine, Ala: Alanine, Mimyo-inositol, Glu: Glutamine, lac: Lactate, ROC: Receiver operating characteristic

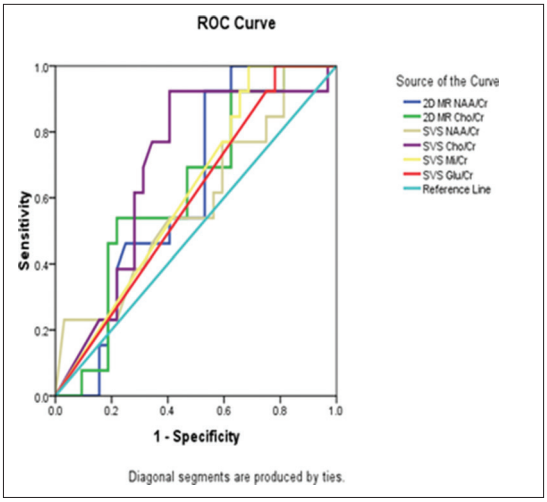

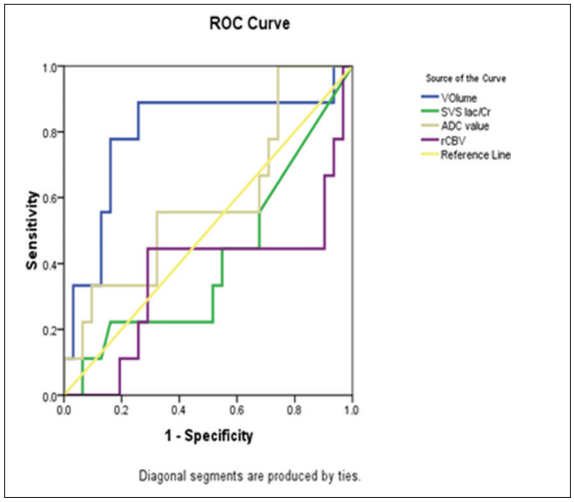

from different areas of tumoral, and normal-appearing mirrored areas showing the greatest visually identifiable CBV values on color maps. The regions were defined as[1] normal tissue-an area containing no enhancement, normal signal intensity on T2/fluid attenuated inversion recovery (FLAIR) images;[2] tumoral area-a region containing clearly well-defined solid portion, preferably uniform contrast enhancement, and high signal intensity on T2/FLAIR images; and to provide the highest reproducibility in CBV measurements, macroscopic cystic/necrotic areas, cerebrospinal fluid-filled sulci or cisterns, and major vessels were avoided. The area of regions of interest was kept nearly constant to minimize confounding factors in the rCBV analysis. The highest CBV value out of five regions of interest was recorded for each area. It was necessary to express the measurement relative to a standard reference, which was called rCBV. The values obtained from tumoral and normal areas were recorded for statistical analysis. We did correlation with histopathology results to compare, benign versus malignant, low grade versus high grade, and different tumor types.

Data were expressed as mean ± standard deviation (SD) and median (range) and Kolmogorov–Smirnov analysis were used to check distribution. Fischer exact test or Chi-square test was used to check the significance of the difference between the frequency distribution of data in different groups. Kruskal–Wallis test followed by *post hoc* Bonferroni's tests was used to study the significance of the difference between more than two groups in case of nonparametric data. ANOVA followed by *post hoc* Tukey's honestly significant difference test was used to study the significance of the difference between more than two groups in case of parametric data. $P < 0.05$ was considered to be statistically significant. Sample size exceeded the required sample size calculated for the power of the study 0. 8, α error to be 0.05, and the population means as seen in the previous study. SPSS ®14 (IBM Corp. NY, USA) and MS Excel® (Microsoft Corp. New Mexico, USA) were used for statistical calculations. Receiver operating characteristic curve was plotted to check for diagnostic significance.

Table 8: Diagnostic potential and diagnostic cutoff of various radiological parameters to diagnose astrocytoma from non-astrocytic intraaxial tumors

AUC								
Test result variable (s)	AUC	Std. error[a]	*P* value	Asymptotic 95% CI		Cutoff	Sensitivity	Specificity
				Low	High			
2D MR NAA/Cr[a]	0.626	0.083	0.189	0.464	0.788	0.73	92.3	40.6
2D MR Cho/Cr[a]	0.625	0.087	0.193	0.454	0.796	2.95	53.8	78.1
SVS NAA/Cr[a]	0.587	0.095	0.367	0.401	0.772	0.045	23.1	96.9
SVS Cho/Cr[a]	0.697	0.085	0.040	0.531	0.864	3.78	92.3	59.4
SVS Mi/Cr[a]	0.620	0.085	0.211	0.454	0.787	1.96	100	31.2
SVS Glu/Cr[a]	0.594	0.088	0.329	0.421	0.766	1.81	100	21.9
Volume[b]	0.796	0.099	0.008	0.602	0.989	47.82	88.9	74.2
SVS Iac/Cr[b]	0.410	0.111	0.418	0.192	0.628	3.955	22.2	83.9
ADC value[b]	0.591	0.112	0.409	0.372	0.810	745.5	100	25.8
rCBV[b]	0.366	0.121	0.225	0.128	0.604	3.32	44.4	71.0

[a]: Positive if lesser than or equal to, [b]: Positive if greater than or equal to, rCBV: Relative cerebral blood volume, Adc: Apparent diffusion coefficient, ROI: Region of interest, EPI: Echo-planar imaging, TSIC: Time signal intensity curve, SVS: Single-voxel spectroscopy, 2D-MVS: 2D multivoxel spectroscopy, NAA: N-acetyl aspartate, Cho: Choline compounds, Cr: Creatine, Ala: Alanine, Mimyo-inositol, Glu: Glutamine, lac: Lactate, ROC: Receiver operating characteristic, AUC: Area under the curve

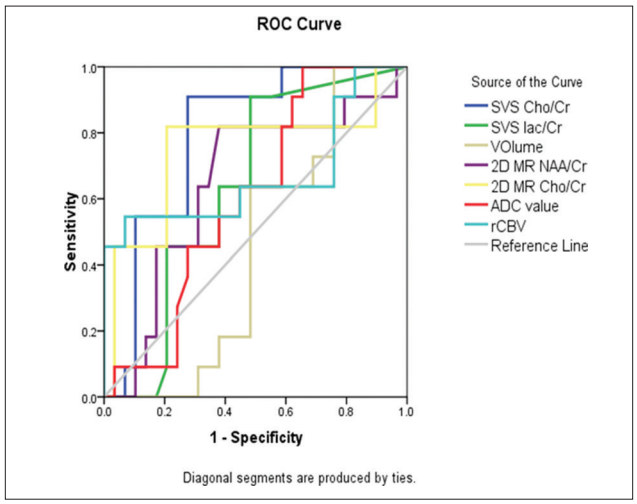

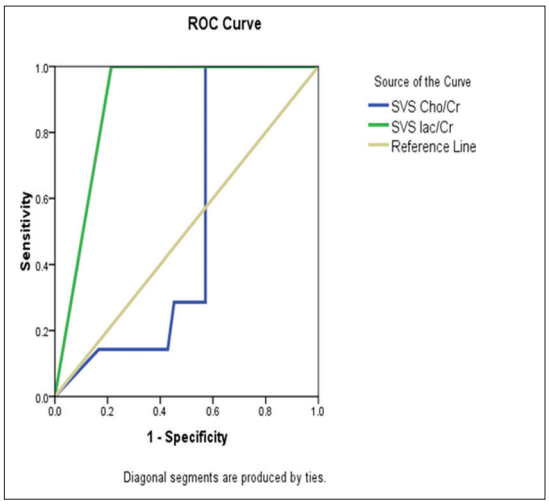

OBSERVATIONS AND RESULTS

In this study, we assessed 70 patients having primary or metastatic brain tumors. We classified tumors into two major groups, primary and metastatic brain tumors out of which primary is again classified into two groups, i.e., intraaxial and extraaxial tumors. Intraaxial tumors were again differentiated into three groups as astrocytoma oligodendroglioma and other intraaxial tumors. Central neurocytoma, choroid plexus tumors, and hemangioblastoma were included in other intraaxial tumors. The extraaxial tumors were further divided into meningothelial and non-meningothelial tumors.

The study included 33 male and 37 female subjects. The mean age is 38.67 years (SD. 17.79). Out of 70, there were 30 astrocytic tumors, three oligodendroglial tumors, nine cranial nerve tumors, 15 meningothelial tumors, and five metastatic tumors which were assessed in terms of ADC value, spectroscopic ratios in relation to Cr, rCBV, and TSIC as shown in Table 1.

When different parameters were compared between types of tumors, significant difference was noted between tumors regarding Volume, 2D MR NAA/Cr, 2D MR Cho/Cr, SVS Cho/Cr, SVS Iac/Cr, SVS Mi/Cr, SVS Glu/Cr, ADC value, and rCBV [Figure 1]. On further *post hoc* analysis, volume was found to be significantly higher in oligodendroglial tumors compared to all other tumors [Table 2]. 2D MR NAA/Cr was found to be significantly lower in astrocytic tumors, meningothelial tumors, metastasis, and oligodendroglial tumors compared to cranial nerve tumors. 2D MR Cho/Cr was found to be significantly lower in Astrocytic tumors compared to meningothelial tumors. ADC value was found to be significantly lower in metastasis compared to astrocytic tumors and meningothelial tumors.

Comparison of various radiological parameters between subjects with different grades of the tumor showed a significant difference was noted in volume, SVS NAA/Cr, SVS Cho/Cr, SVS Mi/Cr, and ADC value [Table 3]. On *post hoc* analysis, SVS Cho/Cr was found to be significantly less in

Table 9: Diagnostic potential and diagnostic cutoff of various radiological parameters to differentiate schwannoma from meningo epithelial tumors

AUC								
Test result variable (s)	Area	Std. error[a]	Asymptotic sig.[b]	Asymptotic 95% confidence interval		Cutoff	Sensitivity	Specificity
				Lower bound	Upper bound			
Volume[a]	0.557	0.150	0.696	0.263	0.851	40.40	71.4	70
2D MR NAA/Cr[b]	0.143	0.092	0.015	-0.038	0.324	0.73	100	63.3
2D MR Cho/Cr[a]	0.800	0.126	0.040	0.552	1.048	4.49	100	80
SVS NAA/Cr[b]	0.307	0.144	0.188	0.025	0.590	5.65	42.9	100
SVS Cho/Cr[a]	0.914	0.083	0.005	0.751	1.078	4.69	100	90
SVS lac/Cr[a]	0.950	0.059	0.002	0.835	1.065	0.255	100	90
SVS Mi/Cr[b]	0.171	0.117	0.025	-0.057	0.400	2.17	85.7	90.9
SVS Glu/Cr[b]	0.243	0.131	0.079	-0.014	0.500	4.29	71.4	90.9
ADC value[a]	0.643	0.143	0.329	0.362	0.923	1022	85.7	60
rCBV[a]	0.629	0.148	0.380	0.339	0.918	5.255	100	60

The test result variable (s): SVS NAA/Cr, SVS lac/Cr, SVS Mi/Cr, and SVS Glu/Cr have at least one tie between the positive actual state group and the negative actual state group. Statistics may be biased. [a]: Under the nonparametric assumption, [b]: Null hypothesis: True area = 0.5, AUC: Area under the Curve, CBV: Relative cerebral blood volume, Adc: Apparent diffusion coefficient, ROI: Region of interest, EPI: Echo-planar imaging, TSIC: Time signal intensity curve, SVS: Single-voxel spectroscopy, 2D-MVS: 2D multivoxel spectroscopy, NAA: N-acetyl aspartate, Cho: Choline compounds, Cr: Creatine, Ala: Alanine, Mimyo-inositol, Glu: Glutamine, lac: Lactate, ROC: Receiver operating characteristic

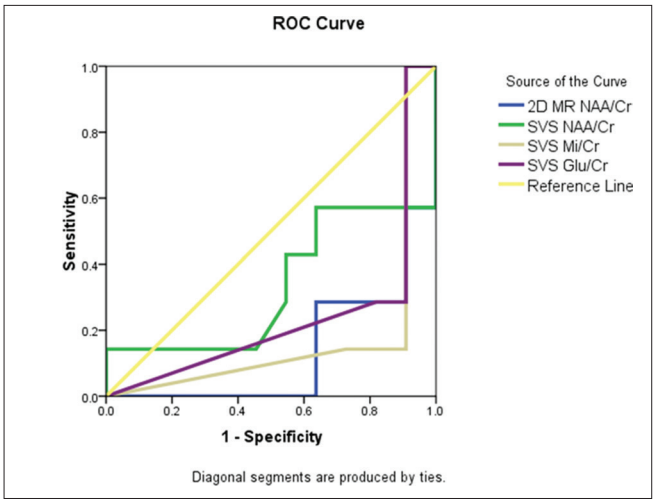

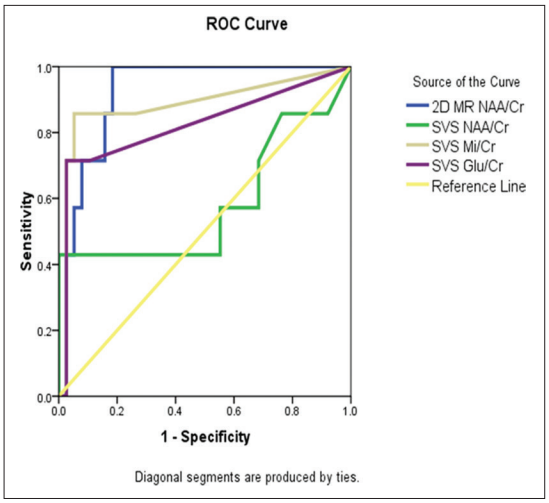

metastasis lesions compared to Grade I tumor. ADC value was found to be significantly less in Grade II, Grade III, Grade IV, and metastasis tumors compared to Grade I also Grade IV and metastasis was found to be having significantly lower ADC value compared to Grade II tumor.

Comparison of various radiological parameters between astrocytic tumors and non-astrocytic tumors is shown in Table 4. Volume was found to be significantly larger ($P = 0.003$) and 2D MR Cho/Cr was found to be significantly lower ($P = 0.007$) in case of Astrocytic tumors. Significant associating was detected between different classes and grades of tumors in relation to TSIC [Table 5].

DISCUSSION

Our study demonstrated that with the variable combination of mean ADC value, rCBV and MR spectroscopy can significantly differentiate types and grades of brain tumors. Starting with a primary and metastatic tumor, our study shows a significant difference in ADC values between the two groups ($P < 0.05$) [Table 2]. Primary brain tumors have higher ADC value as compared to metastasis,[1] but cannot differentiate high-grade gliomas from lymphoma or lymphoma from metastasis.[2]

A significant difference ($P < 0.05$) [Table 2] was also noted in NAA/Cr and Cho/Cr ratios, which were significantly lower in metastasis than primary brain tumors. Cho/Cr ratio in the tumoral area was significantly lower in low-grade tumors than in high-grade tumors and metastasis; no significant difference was seen between primary high-grade tumors and metastasis.[3,4]

Extraaxial tumors are characterized by a near complete absence of neuronal marker NAA[5] [Table 6]. There is a significant difference with short TE as well as long TE while

comparing Cr, Gly, Mi, choline, and lipid between metastasis and gliomas.[6] At short TE, intratumoral Cr suggestive of glioma while its absence favors metastasis.[7] A significant difference was present in the spectroscopic value of NAA/Cr, Cho/Cr, and Cho/NAA ratios between low-grade gliomas, high-grade gliomas, and metastasis in tumoral and peri-tumoral region.[8] Moreover, the peri-tumoral soft tissue shows altered spectroscopic patterns in case of glioma as compared to metastasis as these lesions have peri-tumoral infiltration, which is not seen in metastasis.[9] We found a significant difference ($P < 0.05$) in Mi/Cr and Glu/Cr ratios on SVS between extraaxial and intraaxial brain tumors, where those ratios were significantly low in subjects with intraaxial brain tumors compared to extraaxial tumors [Table 6]. A significant difference in the form of higher Mi/Cr ratio in extraaxial lesions such as hemangiopericytoma and meningioma compared to intraaxial tumors.[10] Very low Mi and Cr were noted in meningioma as compared to astrocytic tumors.[11] Significant differences were noted in terms of Ala, glycine, Gly, Mi, and Cr.[6]

A separate analysis of radiological parameters of astrocytoma and meningioma was done which showed significantly reduced 2D MR Cho/Cr in astrocytic tumors compared to meningothelial tumors. Strongest predictors were found to be SVS Cho/Cr and 2DMR Cho/Cr. Cho/Cr value ≤3.78 suggest astrocytoma at a sensitivity and specificity of 92.3% and 59.4%, respectively [Table 7]. A lower Cr and inositol in meningiomas than in astrocytomas were observed and also found that malignant astrocytomas are more regionally heterogeneous than meningiomas or benign astrocytomas.[12]

Overall comparison of rCBV among all categories of tumors showed a significant difference ($P = 0.038$) [Table 1] but comparing rCBV between any two groups including a comparison of astrocytoma with non-astrocytic intraaxial tumors showed no significant difference and needs to be assessed with larger sample size. One study showed a significant difference in rCBV between astrocytoma and oligodendroglioma with cutoff value of 3.0 at a sensitivity and specificity of 100% and 87.5%, respectively.[13]

The NAA/Cr ratios were found to be significantly higher ($P < 0.05$) [Tables 4 and 8] in non-astrocytic intraaxial tumors in comparison to astrocytoma. Shah *et al.* found very high levels of choline surpassing gliomas in central neurocytomas along with the presence of glycine and Ala with the absence of lipids.[14]

ADC values were $P < 0.05$ [Table 3], significantly lower in Grade III astrocytoma as compared to Grades I and II. Similar

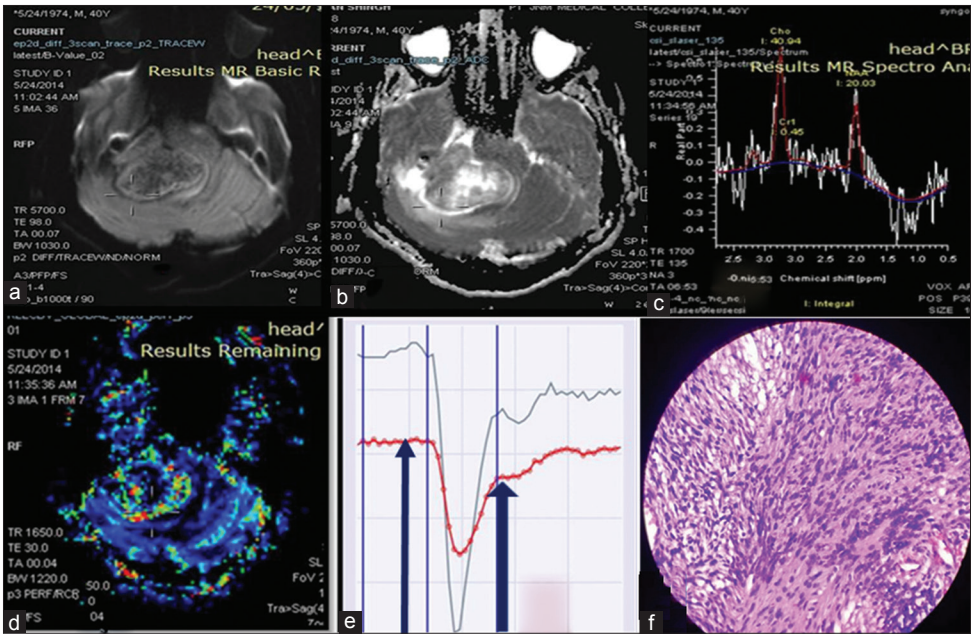

Figure 1: A 40-year-old male patient presented with progressive hearing loss. Figure 1 shows pre-operative magnetic resonance (MR) imaging of the patient. (a) Diffusion weighted image at b value 1000 show focal areas of diffusion restriction with corresponding low apparent diffusion coefficient (b). (c) 2D proton MR spectroscopy shows markedly increase choline with a decrease in N-acetyl aspartate. (d) Relative change in relative cerebral blood volume (rCBV) of tumor tissue as compared to the normal appearing parenchyma in the form of color code maps (rCBV = 2.1). (e) Time signal intensity mean curve in which red line shows approximately 80% regain in signal intensity of tumoral tissue. Histopathology shows predominantly hypercellular area (Antoni A area). Cells are narrow, elongated, and wavy with tapered ends interspersed with collagen fibers. (f). Nuclear palisading around the fibrillary process (Verocay bodies) is seen (hematoxylin-eosin, × 400) suggestive of Schwannoma

findings were observed in one study which also concluded that minimum ADC and ADC difference helps in accurate diagnosis of grades of astrocytoma.[15] We also found ADC values were found to be significantly lower in Grade IV

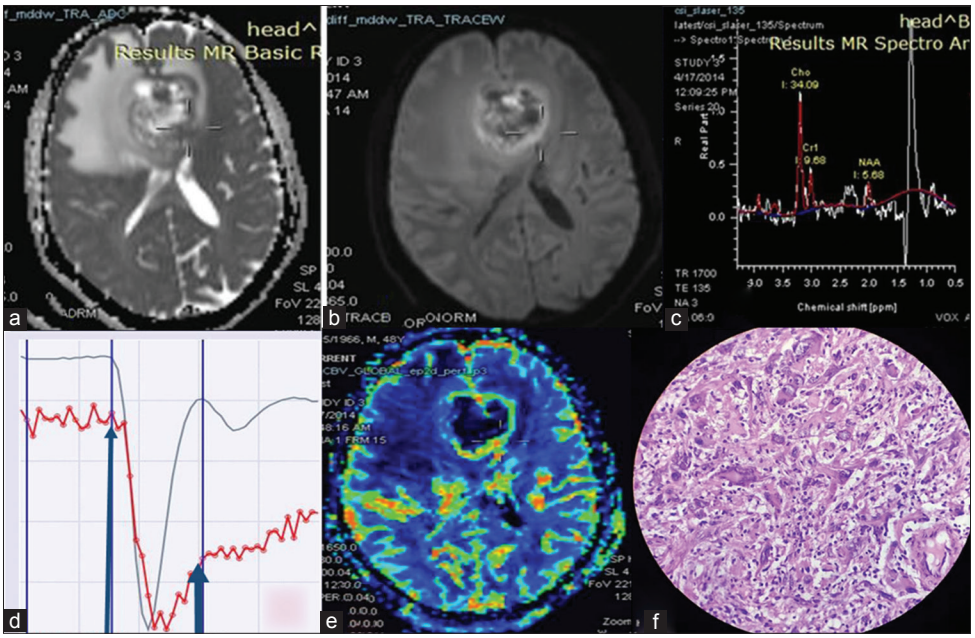

Figure 2: A 48-year-old male patient presented with progressively increasing headache. Pre-operative magnetic resonance (MR) imaging of the patient shows the peripheral area of diffusion restriction (a) at b value 1000 with corresponding low apparent diffusion coefficient (b) and also differentiating it from perilesional edema. (c) 2D proton MR spectroscopy shows significantly increase Choline/Creatine ratio with markedly decrease N-acetyl aspartate and a large lipid peak at 1.3 ppm. (d) Perfusion time signal intensity curve showing 20–40% regain in the signal intensity (red line). (e) Tumor has higher relative cerebral blood volume than normal appearing parenchyma. (f) Histopathological section from excision biopsy shows malignant glial tumor having pleomorphic and bizarre tumor cell along with multinucleated tumor giant cells (hematoxylin-eosin, × 400) suggestive of gliosarcoma

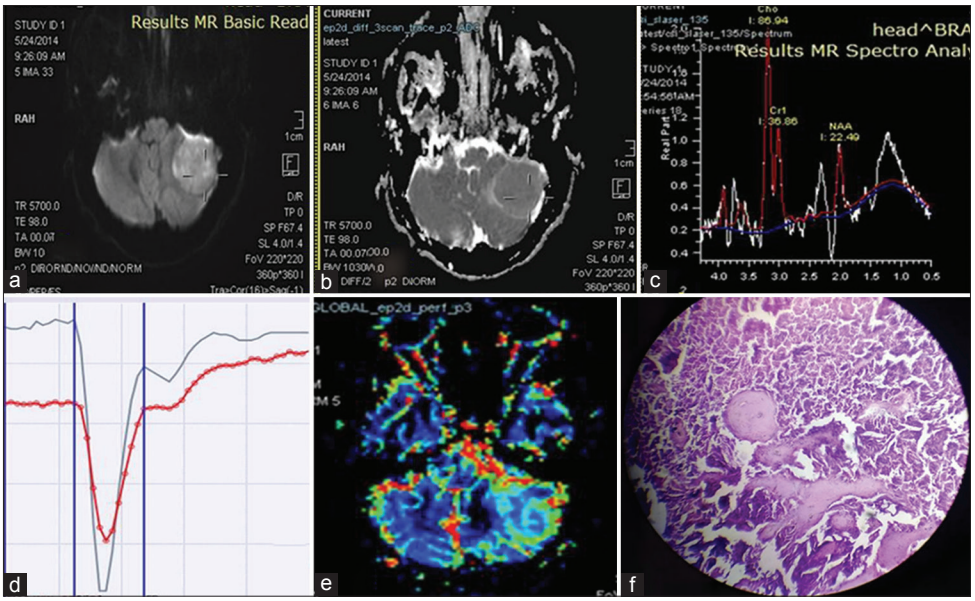

Figure 3: A 45-year-old female having a history of Bidi (a kind of tobacco) smoking since 20 years presented with complaints of chronic headache and single episode of loss of consciousness. Cerebellar signs were present on clinical examination. Figure 3 shows pre-operative magnetic resonance (MR) imaging showing no obvious diffusion restriction (a) with normal apparent diffusion coefficient (b). (c) 2D proton MR spectroscopy showed Choline/Creatine ratio of 2.4 and N-acetyl aspartate/Creatine ~ 0.6. Time signal intensity curve (d) normal regain of signal intensity on first pass. (e) Mildly increased relative cerebral blood volume as compared to normal parenchyma. Histopathological examination shows meningeal tumor composed of spindle cell with indistinct cell boundaries arranged in a sheet such as architecture and whorling pattern. (f) (hematoxylin-eosin, × 400) suggestive of fibroblastic meningioma

tumors than Grades I and II tumors ($P < 0.01$) [Table 2]. A significant negative correlation existed between ADC and astrocytic tumors of the World Health Organization grades 2–4 (Grade 2 vs. Grades 3 and 4, accuracy of 91.3% [$P < 0.01$]; Grade 3 vs. 4, accuracy of 82.4% [$P < .01$]) similar to other studies[16-18] The mean ADC value of normal brain was found to be 0.85×10^{-3} mm^2/s with a significant difference from glial tumors.[19] Hu *et al*. reached a cutoff value of 0.7×10^{-3} mm^2/s for differentiating high grade from low-grade gliomas at sensitivity and specificity of 100% and 82.5%, respectively.[20] A cutoff value of 1.47×10^{-3} mm^2/s for differentiating Grade I from higher grades.[15]

The Choline/Cr was significantly high ($P < 0.05$) in Grade IV tumors compared to Grades I and II tumors [Table 2]. The NAA/Cr ratio was significantly higher ($P < 0.05$) in Grade II tumors compared to Grade III tumors. One of the studies found that anaplastic astrocytomas (the WHO Grade III) are found to have higher choline levels compared to low-

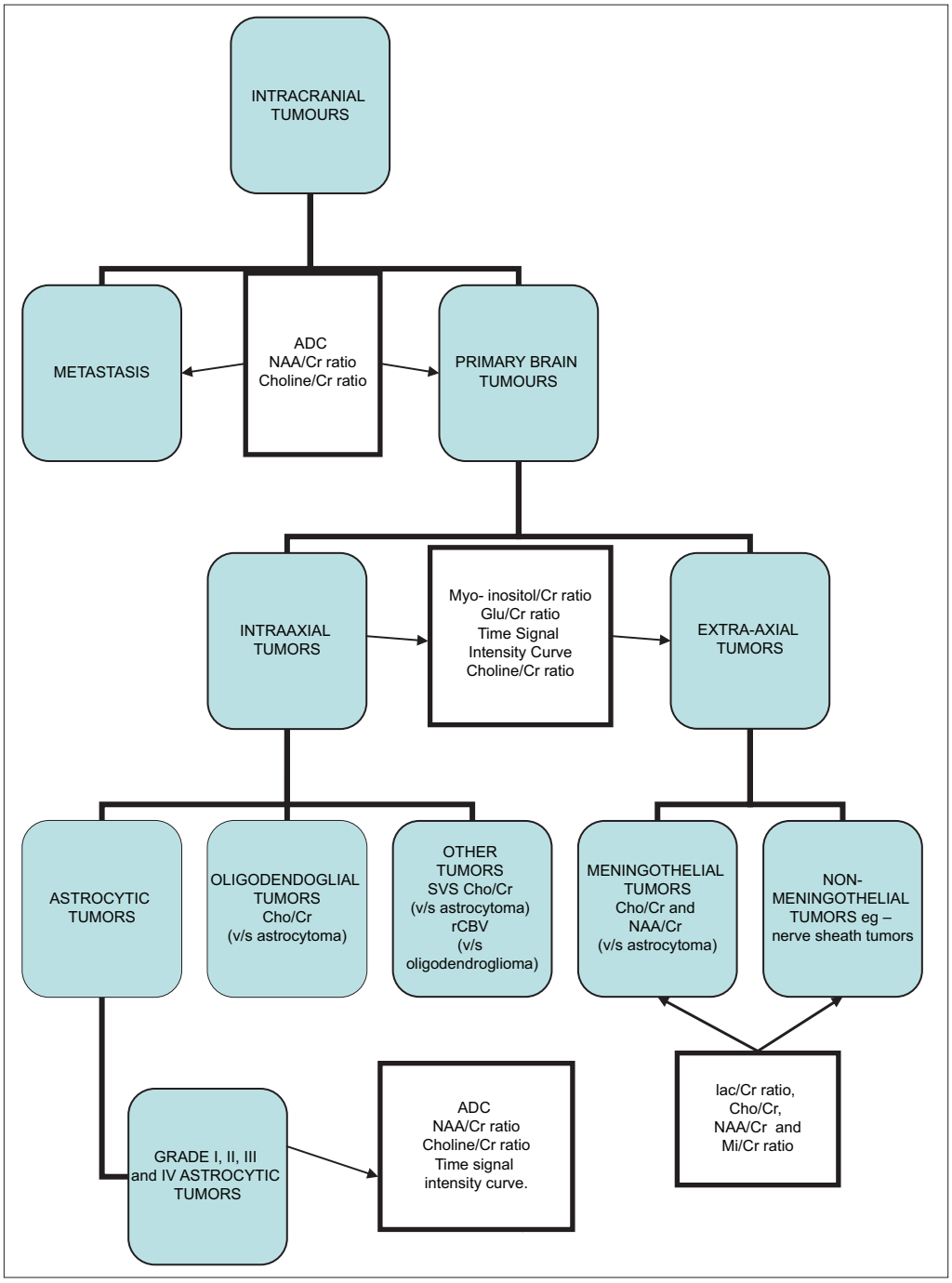

Figure 4: Here, we present an algorithm for approaching brain tumors and systematically approaching to differential diagnosis and obtaining grade of a particular tumor through these physiological magnetic resonance imaging

grade gliomas. A ratio of NAA/Cr has been suggested to accurately discriminate between low and high grade (Grade III) astrocytomas with ratio<1.6 predicting high-grade gliomas.[21] Cho/Cr ratio was also significantly higher in high-grade gliomas.[22]

Mean rCBV ratios were 4.90 ± 1.01 for glioblastomas, [Figure 2] 3.97 ± 0.56 for anaplastic gliomas and 1.75 ± 1.51 for low-grade gliomas, and were thus significantly different.[23] In general, high-grade gliomas have higher rCBV ratios than their counterpart.[24,9] Our study was inconclusive between individual groups, and further evaluation is needed. Evaluation base on signal intensity ratios showed that all tumor spectra differed from spectra of healthy brain tissue similar to other studies.[3,25] TSIC in dynamic susceptibility contrast appears to be a parameter that helps in differentiating intracerebral malignant lesions such as GBM, metastases, and lymphoma.[26] Microvessels within tumors of extra-axial and non-glial origin do not form a blood-brain barrier (BBB) but glioma microvessels form a BBB that is impaired but not absent, the TIC returns toward the baseline in these tumors, but not as much as in the normal brain.[27] We obtained significant difference TSIC while comparing astrocytoma from others, intraaxial from extraaxial and different grades of tumors [Table 5].

The significant difference noted between meningioma and schwannoma [Figures 1 and 3] in terms of Mi/Cr, lac/Cr, Cho/Cr with a sensitivity of 85.7%, 100%, and 100% and specificity of 90%, 90%, and 90.9%, respectively [Table 9]. There is significantly increased Mi/Cr ratio in schwannoma as compared to meningioma in a similar study.[28] Various studies also showed significantly increased Ala in meningioma.[3]

We propose an algorithm with the help of physiological MR sequences for assessment of common brain tumors in addition to conventional MR sequences [Figure 4].

CONCLUSION

Physiological MRI sequences significantly help in identifying type and grades of tumor thereby improving diagnosis and management.

REFERENCES

1. Caravan I, Ciortea CA, Contis A, Lebovici A. Diagnostic value of apparent diffusion coefficient in differentiating between high-grade gliomas and brain metastases. Acta Radiol 2018;59:599-605.
2. Server A, Kulle B, Maehlen J, Josefsen R, Schellhorn T, Kumar T, *et al.* Quantitative apparent diffusion coefficients in the characterization of brain tumors and associated peritumoral edema. Acta Radiol 2009;50:682-9.
3. Kugel H, Heindel W, Ernestus RI, Bunke J, du Mesnil R, Friedmann G, *et al.* Human brain tumors: Spectral patterns detected with localized H-1 MR spectroscopy. Radiology 1992;183:701-9.
4. Dawoud MA, Sherif MF, Eltomey MA. Apparent diffusion coefficient and magnetic resonance spectroscopy in grading of malignant brain neoplasms. Egypt J Radiol Nuclear Med 2014;45:1215-22.
5. Möller-Hartmann W, Herminghaus S, Krings T, Marquardt G, Lanfermann H, Pilatus U, *et al.* Clinical application of proton magnetic resonance spectroscopy in the diagnosis of intracranial mass lesions. Neuroradiology 2002;44:371-81.
6. Majós C, Julià-Sapé M, Alonso J, Serrallonga M, Aguilera C, Acebes JJ, *et al.* Brain tumor classification by proton MR spectroscopy: Comparison of diagnostic accuracy at short and long TE. AJNR Am J Neuroradiol 2004;25:1696-704.
7. Kaminogo M, Ishimaru H, Morikawa M, Suzuki Y, Shibata S. Proton MR spectroscopy and diffusion-weighted MR imaging for the diagnosis of intracranial tuberculomas. Report of two cases. Neurol Res 2002;24:537-43.
8. Caivano R, Lotumolo A, Rabasco P, Zandolino A, D'Antuono F, Villonio A, *et al* 3 tesla magnetic resonance spectroscopy: Cerebral gliomas vs. Metastatic brain tumors. Our experience and review of the literature. Int J Neurosci 2013;123:537-43.
9. Law M, Yang S, Babb JS, Knopp EA, Golfinos JG, Zagzag D, *et al.* Comparison of cerebral blood volume and vascular permeability from dynamic susceptibility contrast-enhanced perfusion MR imaging with glioma grade. AJNR Am J Neuroradiol 2004;25:746-55.
10. Salzedo E, Cortes M, Melançon D, Tampieri D. Myoinositol trends in different types of brain lesions. Neuroradiol J 2009;22:16-21.
11. Howe FA, Opstad KS 1H MR spectroscopy of brain tumours and masses. NMR Biomed 2003;16:123-31.
12. Peeling J, Sutherland G. High-resolution 1H NMR spectroscopy studies of extracts of human cerebral neoplasms. Magn Reson Med 1992;24:123-36.
13. Wetzel SG, Cha S, Law M, Johnson G, Golfinos J, Lee P, *et al.* Preoperative assessment of intracranial tumors with perfusion MR and a volumetric interpolated examination: A comparative study with DSA. AJNR Am J Neuroradiol 2002;23:1767-74.
14. Shah T, Jayasundar R, Singh VP, Sarkar C. *In vivo* MRS study of intraventricular tumors. J Magn Reson Imaging 2011;34:1053-9.
15. Murakami R, Hirai T, Sugahara T, Fukuoka H, Toya R, Nishimura S, *et al.* Grading astrocytic tumors by using apparent diffusion coefficient parameters: Superiority of a one versus two-parameter pilot method. Radiology 2009;251:838-45.
16. Yang D, Korogi Y, Sugahara T, Kitajima M, Shigematsu Y, Liang L, *et al.* Cerebral gliomas: Prospective comparison of multivoxel 2D chemical-shift imaging proton MR spectroscopy, echoplanar perfusion and diffusion-weighted MRI. Neuroradiology 2002;44:656-66.
17. Bulakbasi N, Kocaoglu M, Sanal TH, Tayfun C. Dysembryoplastic neuroepithelial tumors: Proton MR spectroscopy, diffusion and perfusion characteristics. Neuroradiology 2007;49:805-12.
18. de Fatima Vasco Aragao M, Law M, Batista de Almeida D, Fatterpekar G, Delman B, Bader AS, *et al.* Comparison of perfusion, diffusion, and MR spectroscopy between low-grade enhancing pilocytic astrocytomas and high-grade astrocytomas. AJNR Am J Neuroradiol 2014;35:1495-502.
19. Tan FC, Gokoglu A, Tucer B, Caner Y. The apparent diffusion coefficient in glial tumors. OMICS J Radiol 2017;6:256.
20. Hu YC, Yan LF, Wu L, Du P, Chen BY, Wang L, *et al.* Intravoxel incoherent motion diffusion-weighted MR imaging of gliomas: Efficacy in preoperative grading. Sci Rep 2014;4:7208.
21. Verma A, Kumar I, Verma N, Aggarwal P, Ojha R. Magnetic resonance spectroscopy - revisiting the biochemical and molecular milieu of brain tumors. BBA Clin 2016;5:170-8.
22. Lee EJ, Lee SK, Agid R, Bae JM, Keller A, Terbrugge K, *et al.* Preoperative grading of presumptive low-grade astrocytomas on MR imaging: Diagnostic value of minimum apparent diffusion coefficient. AJNR Am J Neuroradiol 2008;29:1872-7.
23. Lee SJ, Kim JH, Kim YM, Lee GK, Lee EJ, Park IS, *et al.* Perfusion MR imaging in gliomas: Comparison with histologic tumor grade. Korean J Radiol 2001;2:1-7.
24. Hakyemez B, Erdogan C, Ercan I, Ergin N, Uysal S, Atahan S, *et al.* High-grade and low-grade gliomas: Differentiation by using perfusion MR imaging. Clin Radiol 2005;60:493-502.
25. Dowling C, Bollen AW, Noworolski SM, McDermott MW, Barbaro NM,

Day MR, *et al.* Preoperative proton MR spectroscopic imaging of brain tumors: Correlation with histopathologic analysis of resection specimens. AJNR Am J Neuroradiol 2001;22:604-12.
26. Hartmann M, Heiland S, Harting I, Tronnier VM, Sommer C, Ludwig R, *et al.* Distinguishing of primary cerebral lymphoma from high-grade glioma with perfusion-weighted magnetic resonance imaging. Neurosci Lett 2003;338:119-22.
27. Rollin N, Guyotat J, Streichenberger N, Honnorat J, Tran Minh VA, Cotton F, *et al.* Clinical relevance of diffusion and perfusion magnetic resonance imaging in assessing intra-axial brain tumors. Neuroradiology 2006;48:150-9.
28. Cho YD, Choi GH, Lee SP, Kim JK. (1)H-MRS metabolic patterns for distinguishing between meningiomas and other brain tumors. Magn Reson Imaging 2003;21:663-72.

How to cite this article: Jain D, Netam SBS, Patre V, Amle D, Sahu R, Gahine R. Role of Diffusion-weighted Imaging, Perfusion Magnetic Resonance Imaging, and Magnetic Resonance Spectroscopy in Evaluating Histopathologically Confirmed Brain Tumors in 3-Tesla Magnetic Resonance Imaging. Int J Sci Stud 2019;7(2):24-37.

Source of Support: Nil, **Conflict of Interest:** None declared.